Intensity liquid level sensor based on multimode interference and fiber Bragg grating

2016 Meas. Sci. Technol. 27 125104

(http://iopscience.iop.org/0957-0233/27/12/125104)

IOP Publishing Measurement Science and Technology
Meas. Sci. Technol. **27** (2016) 125104 (6pp) doi:10.1088/0957-0233/27/12/125104

Intensity liquid level sensor based on multimode interference and fiber Bragg grating

Ricardo Oliveira[1,2], Stenio Aristilde[1], Jonas H Osório[1], Marcos A R Franco[3], Lúcia Bilro[2,4], Rogério N Nogueira[2] and Cristiano M B Cordeiro[1]

[1] Instituto de Física 'Gleb Watagin', Universidade Estadual de Campinas, UNICAMP, Campinas - SP, Brazil
[2] Instituto de Telecomunicações, Pólo de Aveiro, Aveiro, Portugal
[3] Departamento de Ciência e Tecnologia Aeroespacial, Instituto de Estudos Avançados, IEAv, S. J. Campos, Brazil
[4] I3N/FSCOSD—Institute of Nanostructures, Nanomodelling and Nanofabrication, Department of Physics, University of Aveiro, Aveiro, Portugal

E-mail: oliveiraricas@av.it.pt

Received 9 May 2016, revised 26 September 2016
Accepted for publication 29 September 2016
Published 28 October 2016

Abstract

In this paper an intensity liquid level sensor based on a single-mode—no-core—single-mode (SMS) fiber structure together with a Bragg grating inscribed in the later single mode fiber is proposed. As the no-core fiber is sensitive to the external refractive index, the SMS spectral response will be shifted related to the length of no-core fiber that is immersed in a liquid. By positioning the FBG central wavelength at the spectral region of the SMS edge filter, it is possible to measure the liquid level using the reflected FBG peak power through an intensity-based approach. The sensor is also self-referenced using the peak power of another FBG that is placed before and far from the sensing part. The temperature error analysis was also studied revealing that the sensor can operate in environments where the temperature changes are minimal. The possibility to use a second setup that makes the whole device temperature insensitive is also discussed.

Keywords: fiber Bragg grating (FBG), no-core fiber (NCF), liquid level sensor, multimode interference (MMI)

(Some figures may appear in colour only in the online journal)

1. Introduction

Liquid-level sensing is a requirement in many applications such as fuel storage, liquids quantitative and qualitative monitoring and chemical processing. Nowadays, liquid level can be detected with various traditional mechanical or electrical methods. Among them are the float, ultrasonic [1], magnetostrictive [2], differential pressure [3], and capacitive methods [4], etc. However, they present several disadvantages such as high maintenance cost, susceptibility to electromagnetic interference, structure complexity and low resolution. Nevertheless, their application can be compromised if the liquid to be measured is conductive, potentially explosive or erosive. Optical fiber sensors appear as a promising technology to solve many of these problems, since they are made of dielectric and therefore they are non-conductive and cannot be eroded by most of the liquids. Additionally, these sensors can offer multiplexing capabilities, compact size, high resolution and immunity to electromagnetic interference.

To date, several optical fiber liquid level sensors have been reported on literature, where the key concept relies on the interaction of the evanescent field of the optical signal with the liquid refractive index (RI). This has been done by using long period gratings [5], etched fibers [6], D-shape fibers [7], and also multimode fiber devices (MMI) based on unclad multimode fibers [8–11]. In fact, some of these sensors are

based on complex fabricating procedures or elaborate device structures. Additionally, the measurement concept on most of the fiber optic liquid level sensors relies on the wavelength dependency, which therefore, needs an expensive optical detection system to recover the liquid level.

Regarding MMI fiber based sensors, apart from measuring liquid level based on the change of the resonance wavelength, they have been used in special arrangements to detect individually or simultaneously a variety of parameters, such as: temperature, refractive index [12–14], strain [15, 16], vibration [17], bending [16], magnetic field [18], and displacement [19]. For the refractive index detection, as it occurs for the liquid level detection, it is necessary to expose the fiber core to the external environment. This can be done with a multimode fiber (MMF) composed of a single material commonly known as no-core-fiber (NCF), or by simply etching the cladding of a MMF [14]. In fact, fiber based MMIs are a simple device that comprises a single-mode—multimode—single-mode structure (SMS), which allows easy and compact implementation. On the other hand fiber Bragg gratings (FBGs) are a common sensing device widely used in sensing applications [20]. The potential of combining these fiber structures has already been subject of study in literature [11–16, 18, 21]. Although, none of these studies has reported the capability to measure liquid level based on the peak power of an FBG.

In this work, we propose the combination of a SMS structure based on a NCF together with a single mode FBG to measure liquid level. The measurement principle is based on the detection of the FBG reflected peak power offering, thus, an easy characterization method. The dependence of temperature on the FBG peak power was also subject of study in this work.

2. Principle of operation

The experimental setup and schematic of the sensor are shown on figure 1.

The sensor shown on the inset of figure 1 is composed of a NCF which is a pure silica rod with 125 μm diameter, sandwiched between two single-mode fibers (SMF), where the later SMF has an FBG inscribed on it. Considering the SMS structure in air, multiple modes will be excited when the fundamental mode of the leading SMF is injected on the NCF. As these modes have different propagation constants, they will interfere as they propagate along the NCF. This will allow the formation of multiple images of the input field, which are an exact replica of both phase and amplitude. The length in which these images are formed can be obtained from the restricted symmetric interference condition [22], which is given by:

$$L = p\frac{3L_\pi}{4}, \quad p = 0, 1, 2, 3 \tag{1}$$

with L_π defining the beat length [22], expressed as:

$$L_\pi \approx \frac{4n_{\mathrm{NCF}}D_{\mathrm{NCF}}^2}{3\lambda_0} \tag{2}$$

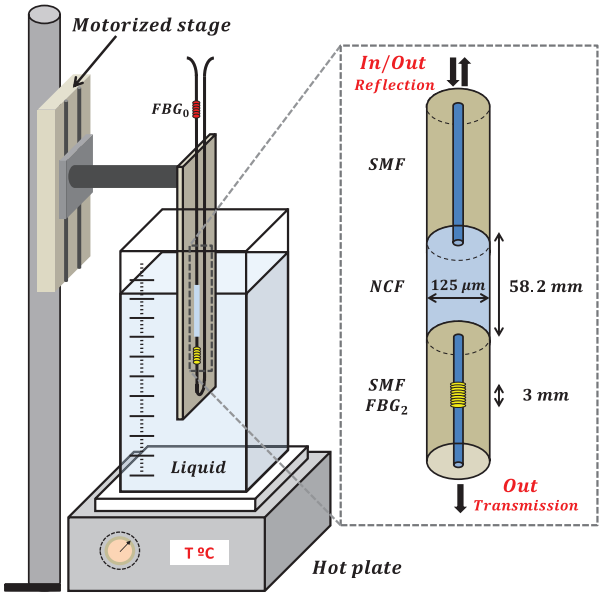

Figure 1. Setup used for the sensor characterization, composed of a motorized linear stage that controls the sensor height on a water container with controlled temperature. The inset shows the sensor parts, composed by the SMS structure and FBG.

where λ_0 is the free space wavelength, with n_{NCF} and D_{NCF}, respectively the effective refractive index and diameter of the fundamental mode of the NCF considering air as external medium. If the NCF is precisely cleaved where one of the images is being formed, a bandpass filter centered at λ_0 will be formed. The combination of (1) and (2) provides the wavelength at which this filter will be centered:

$$\lambda_0 \approx p\frac{n_{\mathrm{NCF}}D_{\mathrm{NCF}}^2}{L} \tag{3}$$

When the SMS structure is fully immersed in a liquid the refractive index difference between the two media (silica/liquid) is lower when compared with the case where the fiber is in air. Thus, due to the *Goos–Hänchen* effect, the lateral penetration of the field into the liquid will be higher [22]. Consequently, the effective diameter (D_{NCF}), will increase, increasing also the effective refractive index (n_{NCF}), because the evanescent filed penetrates more into the liquid. Consequently, the center wavelength of the bandpass filter expressed in equation (3) will be redshifted [8].

On the other hand, when the NCF is surrounded by two different media (e.g. one part immersed in a liquid and another part in air), the sensor passes to act as the combination of two NCFs, and the center wavelength of the band pass filter will be estimated from equation (4), [8]:

$$\lambda_0 = 4\frac{n_{\mathrm{NCF_{Liq.}}} \times D_{\mathrm{NCF_{Liq.}}}^2}{L}\left(\frac{L_{\mathrm{Liq.}}}{L}\right) + 4\frac{n_{\mathrm{NCF}}D_{\mathrm{NCF}}^2}{L}\left(\frac{L_{\mathrm{air}}}{L}\right), \tag{4}$$

where the first part of the equation refers to the NCF in liquid and the second part refers to the NCF in air. The variables L_{Liq} and L_{air} are respectively the length of the NCF, with and without the liquid; $n_{\mathrm{NCF_{Liq}}}$, $D_{\mathrm{NCF_{Liq}}}$ express the effective

refractive index and diameter of the fundamental mode of the NCF section in liquid.

At this stage and without using the FBG it is possible to use the shift of the center wavelength produced by the MMI bandpass filter to measure liquid level [8, 9, 11]. However, one of the drawbacks of this measurement concept is the large width of a typical MMI spectra that imposes uncertainty on the estimation of the peak wavelength.

Nevertheless, the MMI spectral response can act as a bandpass filter. Therefore, if an FBG is introduced after the NCF and at a specific wavelength region, it is possible to linearly measure the FBG peak power with the external refractive index [13, 14]. This happens, because the SMS structure and FBG are sensitive and insensitive to the external refractive index, respectively. This will be transduced as a relative movement of the MMI spectrum related to the FBG spectrum, imposing power variation on the FBG spectra due to the filtering of the MMI spectra.

It is known that standard FBGs are wavelength insensitive to changes on the external refractive index medium and, so, to the liquid level. On other hand, looking to equation (4), the center wavelength of the bandpass filter of the SMS structure is liquid level dependent. Therefore, using the SMS structure followed by an FBG, one can find that this fiber device allows one to monitor the liquid level by measuring the reflection peak power of the FBG.

3. Experimental setup

The NCF used in this work was produced in our facilities and it has a diameter of 125 μm and a refractive index of 1.444 at 1550 nm. Equation (3) was used to calculate the NCF length needed to get a peak centered at $\lambda_0 = 1550$ nm. In order to have enough length for the manipulation and for the splicing process, it was chosen the 4th self-image ($p = 4$), giving a length of 58.2 mm. The NCF was then measured with a digital caliper and cleaved with a fiber optic cleaver machine. Each end of the NCF was then fusion spliced to a single-mode fiber creating the SMS structure.

3.1. Preliminary tests

In order to define the center wavelength where the grating should be written, it is necessary to find the wavelength regions where the FBG peak power can experience maxima variations on the liquid level detection. Therefore, the SMS structure was subjected to the two opposite conditions, respectively fully in air and fully immersed in liquid (i.e. water). The correspondent spectral responses were acquired with an interrogator system (FS2200—Industrial BraggMETER, FiberSensing) and are depicted on figure 2(a). The correspondent power difference between the two spectra is shown on figure 2(b). As predicted, the MMI spectrum is redshifted when it is immersed in water. The power difference between the spectrum in air and fully immersed in water produces negative and positive power values that can be seen on figure 2(b). Results show that greater power variations are observed around 1535 and 1561 nm.

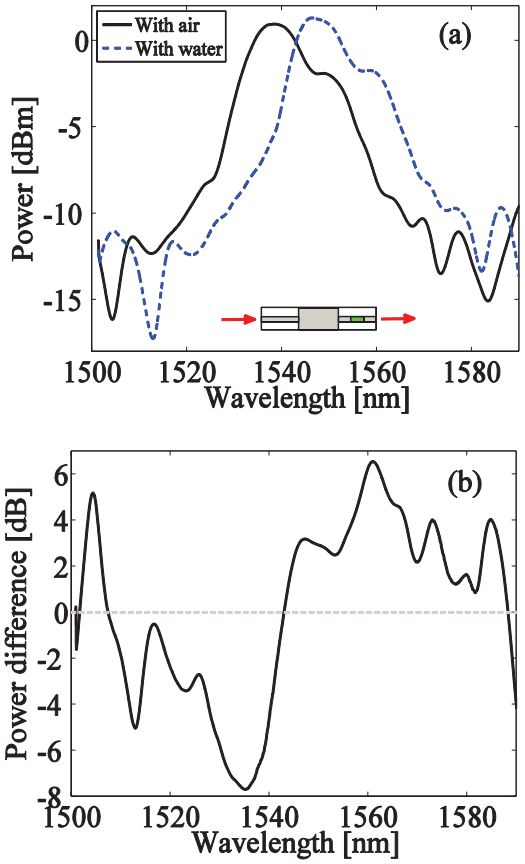

Figure 2. (a) Spectra collected for the SMS structure in air and water; (b) power difference between the spectra in air and water, shown in (a).

Nevertheless, the shape of the MMI spectra acts as a bandpass filter and to get a straight evolution of the FBG peak power with the liquid level, the MMI spectra need to have a straight tendency on the region where the FBG will be written.

3.2. Liquid level detection optimization

Regarding the above observations, we decide to evaluate the wavelength region that maximizes de liquid level detection performance. Thus, the response of the SMS structure was characterized with increments of liquid level, allowing to know the correspondent power values at specific wavelength regions (i.e. 1535 and 1561 nm). To do that, both ends of the fiber sensor where fixed onto a support in a straight position, in order to avoid undesired strain and bend effects on the NCF that may affect the transmission spectrum. The support was therefore attached to a motorized linear stage (LTS300 from Thorlabs), which was used to precisely move the sensor inside a liquid container in a 3 mm step. The container is filled with water and it was placed on top of a hot source (IKA®C-MAG HS7), which kept the temperature constant at 25 °C. This experimental setup can be seen on figure 1. In order to avoid the zones where the fusion splices were made, the characterization was performed at the central part of the SMS structure, covering a range of 51 mm from the total 58.2 mm. The correspondent transmission spectra can be seen on figure 3(a).

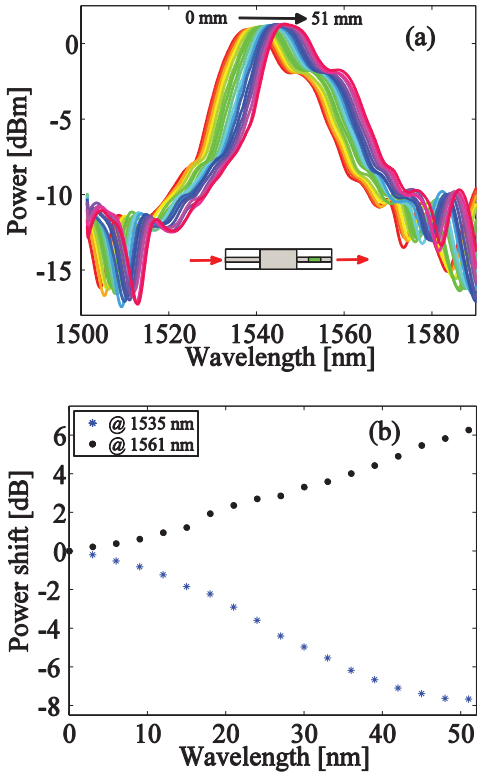

Figure 3. (a) Transmission spectra of the SMS structure, acquired for different positions of the sensor in water. (b) Power acquired from spectra shown in (a), for the two best wavelength regions, respectively at 1535 and 1561 nm.

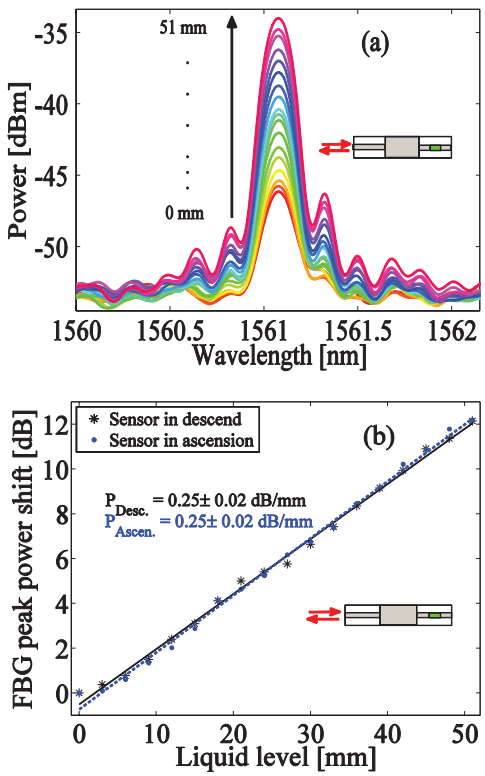

Figure 4. (a) FBG reflection spectra acquired when the sensor is immersed in water in steps of 3 mm; (b) calibrated FBG peak power for different water levels, when the sensor is immersed and removed from water.

From the spectra depicted on figure 3(a), it was possible to determinate the optical power for the two wavelength regions that satisfy the best sensitivity range, respectively at 1535 and 1561 nm (figure 3(b)). Considering the obtained results, one can find that the optical powers obtained at 1561 nm have produced a straighter dependency in a broader range when compared to the values at 1535 nm. For that reason, we decide to inscribe an FBG centered at a region nearby 1561 nm.

3.3. Grating inscription

The Bragg grating was inscribed through the phase mask technique, using a 266 nm UV radiation from a *Quantel Q-Smart 450* laser. The laser repetition rate was set to 10 Hz, with pulse energy of 5 mJ, during 15 min exposure time. The long inscription time is related to the lower photosensitivity of the fiber, which can be reduced by hydrogen load the fiber prior to the inscription process. The grating was inscribed at 1561.2 nm with 3 mm in length and at 60 mm after the NCF, (see the inset of figure 1). Thanks to the multiplexing capabilities offered by the FBG technology, another FBG was written before the NCF and far from the sensing part—FBG_0 in figure 1. This FBG was centered at 1541 nm and will be used for power calibration during the acquisitions since it does not interact with the sensor part.

4. Results and discussions

4.1. Sensor characterization

The sensor characterization was done following the same procedures described before at section 3.2, for the SMS structure. In order to evaluate the hysteresis of the system, two different situations were tested: descending and ascending the sensor on the liquid container.

The correspondent FBG reflection spectra collected when the sensor is being immersed in water (3 mm steps) are shown in figure 4(a).

From figure 4(a), it can be seen that as the liquid level increases there is an increase of the reflection FBG peak power, in accordance with the results depicted on figure 3(b). This FBG peak power is then calibrated with the peak power reference of the FBG_0. The correspondent evolution of the calibrated peak power on the immersion and emersion of the sensor in water, were plotted on figure 4(b). As can be seen, the calibrated FBG peak power evolution follows a linear regression model ($R^2 = 0.998$). The obtained sensitivity was 0.25 dB mm^{-1} with a total optical power variation of 12 dB for an operational range of 51 mm. Considering a detection system with a resolution of 0.02 dB, one can find that the system resolution is 0.08 mm.

Another pertinent issue about this liquid level sensor is the total loss induced by the SMF-NCF-SMF splices. The

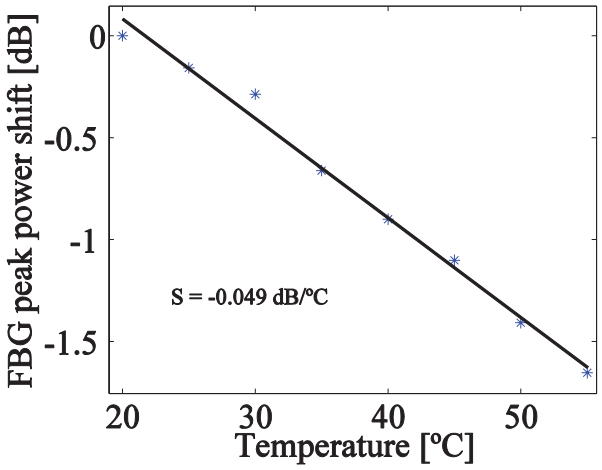

Figure 5. Calibrated FBG peak power shift collected at different temperatures.

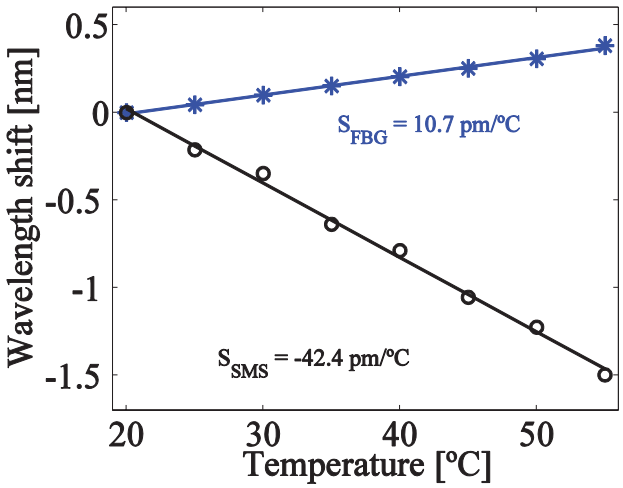

Figure 6. Reflection and transmission peak power wavelength shift evolution for the FBG and SMS structure respectively.

relevance of that is due to the different core diameters and refractive index, which can compromise the system performance. Thus, we estimate that the splicing losses are essentially the loss of the MMI peak power when it is measured in transmission. Since the interrogator has an output power source with 4 dBm and based on the peak power reading of the SMS spectra when it is in air, shown in figure 2(a) (~0.96 dBm), we estimate ~3 dB loss for the two fiber splices (in transmission). Since the sensor operates in reflection (needs to pass two times on the NCF), we estimate a total system loss of ~6 dB.

The NCF length calculated from equation (3), has been chosen to operate the SMS structure at the 4th self-image. Thus, by using an exact multiple of this image, it is possible to use a longer section of the NCF. Therefore, the 12 dB sensing range can be used with a longer NCF fiber, allowing the use of the sensor in a wider range of lengths, with restrictions only in the sensor resolution.

Additionally, the sensor employed on this paper can be constructed in a cost effective way, by just using low cost components as LED and photodetectors, together with a 2×2 fiber coupler for power calibration and signal detection.

4.2. Temperature error analysis

It is know that both FBG and MMI spectral responses are temperature dependent [11–13, 15, 18]. Consequently, this effect may compromise the accuracy of the proposed liquid level sensor under different temperature conditions. Therefore, a temperature test was performed in order to evaluate the measurement uncertainty due to temperature variations. To do that, the fiber based sensor composed by the SMS structure and FBG at 1561 nm was placed on a thermal chamber, where the temperature was raised from 20 to 55 °C, in steps of 5 °C. The correspondent calibrated FBG peak power variations for the different temperatures were determined and they can be seen in figure 5.

Results show that the FBG peak power was linearly blue shifted with increasing temperature. A linear regression model was applied to the experimental data points, obtaining a sensitivity of -0.049 dB °C^{-1}. The observed power shift at the different temperatures corresponds to the active filtering produced by the MMI spectra over the FBG spectra, when both parts (SMS structure and FBG) are being affected. The low temperature dependence is thus the result of the different spectra wavelength shifts produced by each part of the sensor (SMS structure and FBG), which have revealed opposite sensitivity contributions (10.7 and -42.4 pm °C^{-1} for the FBG and SMS structure respectively), (see figure 6).

To find the uncertainty on the liquid level detection when temperature is considered (δ_T), the sensitivity found for the temperature characterization (i.e. figure 5) and the one found for the liquid level characterization were used:

$$\delta_T = \frac{0.049\ \text{dB}\ ^\circ\text{C}^{-1}}{0.25\ \text{dB mm}^{-1}} = 0.2\ \text{mm}\ ^\circ\text{C}^{-1} \tag{5}$$

The estimated value can therefore, compromise the accuracy of the proposed sensor at high temperature changes. However, this may be solved by calibrating the signal using a parallel sensor based on the same configuration studied on this paper where the NCF is replaced by a step index MMF. In that way, the parallel sensor will be independent to the liquid level, since the MMF has an outer cladding that avoids the interaction of the light with the external environment. On the other hand, the parallel sensor will be temperature dependent. By using both sensors simultaneously and in real time it is possible to recover the liquid level independent of temperature.

5. Conclusions

We have proposed and demonstrated a simple and reliable liquid level sensor based on the use of a SMS structure and FBG. The detection relies on a self-referenced method that is based on the acquisition of the FBG peak power. The developed sensor can be deployed in a low cost solution based on an optical source centered at the FBG together with a photodetector a fiber coupler.

The sensitivity reported with the proposed sensor was 0.25 dB mm^{-1}. The temperature tests used to verify the temperature influence on the liquid level measurement showed an uncertainty of 0.2 mm $°C^{-1}$, revealing that the sensor can operate in environments where the temperature changes are minimal. Additionally, the sensor can be simply operated in reflection avoiding too much instrumentation.

Acknowledgments

This work was funded by FINEP (#01.12.0393.00) and by FCT-Fundação para a Ciência e Tecnologia through portuguese national funds PEstOE/EEI/LA0008/2013 and UID/EEA/50008/2013 (Swat), PhD Scholarship SFRH/BD/88472/2012, investigator grant IF/01664/2014 and project INITIATE. J H Osório acknowledge CNPq for financial support.

References

[1] Terzic J, Nagarajah C R and Alamgir M 2010 Fluid level measurement in dynamic environments using a single ultrasonic sensor and support vector machine (SVM) *Sensors Actuators* A **161** 278–87

[2] Yibo L, Liying S, Shijiu J and Li B S 2006 Development of magnetostriction sensor for on-line liquid level and density measurement *Proc. World Congr. Intell. Control Autom.* **1** 5162–6

[3] Richter M, Wackerle M, Woias P and Hillerich B 1999 A novel flow sensor with high time resolution based on differential pressure principle *Proc. of the 12th IEEE Int. Conf. on Micro Electro Mechanical Systems (MEMS'99) (Orlando, FL, USA)* pp 118–23

[4] Kumar B, Rajita G and Mandal N 2014 A review on capacitive-type sensor for measurement of height of liquid level *Meas. Control* **47** 219–24

[5] Khaliq S, James S W and Tatam R P 2001 Fiber-optic liquid-level sensor using a long-period grating *Opt. Lett.* **26** 1224–6

[6] Yun B, Chen N and Cui Y 2007 Highly sensitive liquid-level sensor based on etched fiber bragg grating *IEEE Photonics Technol. Lett.* **19** 1747–9

[7] Chandani S M and Jaeger N A F 2007 Optical fiber-based liquid level sensor *Opt. Eng.* **46** 114401–6

[8] Antonio-Lopez J E, Sanchez-Mondragon J J, Likamwa P and May-Arrioja D A 2011 Fiber-optic sensor for liquid level measurement *Opt. Lett.* **36** 3425–7

[9] Antonio-Lopez J E, May-Arrioja D A and LikamWa P 2011 Fiber-optic liquid level sensor *IEEE Photonics Technol. Lett.* **23** 1826–8

[10] Luo Y, Xia L, Yu C, Li W, Sun Q, Wang Y and Liu D 2015 Multi-parameter optical fiber sensor based on enhanced multimode interference *Opt. Commun.* **344** 120–4

[11] Li C, Ning T, Zhang C, Li J, Wen X, Pei L, Gao X and Lin H 2016 Liquid level measurement based on a no-core fiber with temperature compensation using a fiber Bragg grating *Sensors Actuators* A **45** 49–53

[12] Bai Y, Yin B, Liu C, Liu S, Lian Y and Jian S 2014 Simultaneous Measurement of Refractive Index and Temperature Based on NFN Structure *IEEE Photonics Technol. Lett.* **26** 2193–6

[13] Li L, Xia L, Wuang Y, Ran Y, Yang C and Liu D 2012 Novel NCF-FBG interferometer for simultaneous measurement of refractive index and temperature *IEEE Photonics Technol. Lett.* **24** 2268–71

[14] Shao M, Qiao X, Jiasurname Z, Fusurname H, Liu Y, Li H and Zhao X 2015 Refractive index measurement based on fiber Bragg grating connected with a multimode fiber core *Opt. Commun.* **351** 70–4

[15] Zhou D-P, Wei L, Liu W-K, Liu Y and Lit J W Y 2008 Simultaneous measurement for strain and temperature using fiber Bragg gratings and multimode fibers *Appl. Opt.* **47** 1668–72

[16] Sun A and Wu Z 2015 Multimode interference in single mode—multimode FBG for simultaneous measurement of strain and bending *IEEE Sens. J.* **15** 3390–4

[17] Ran Y, Xia L, Han Y, Li W, Rohollahnejad J, Wen Y and Liu D 2015 Vibration fiber sensors based on SM-NC-SM fiber structure *IEEE Photonics J.* **7** 6800607

[18] Li C, Ning T, Wen X, Li J, Zhang C and Zhang C 2015 Magnetic field and temperature sensor based on a no-core fiber combined with a fiber Bragg grating *Opt. Laser Technol.* **72** 104–7

[19] Antonio-Lopez J E, LiKamWa P, Sanchez-Mondragon J J and May-Arrioja D A 2013 All-fiber multimode interference micro-displacement sensor *Meas. Sci. Technol.* **24** 055104

[20] Cusano A, Cutolo A and Albert J 2011 *Fiber Bragg Grating Sensors: Recent Advancements, Industrial Applications and Market Exploitation* (Sharjah: Bentham Science Publishers) (doi: 10.2174/97816080508401110101)

[21] Rong Q, Qiao X, Guo T, Wang R, Zhang J, Hu M, Feng Z, Weng Y and Ma Y 2012 Temperature-calibrated fiber-optic refractometer based on a compact FBG-SMS structure *Chinese Opt. Lett.* **10** 030604

[22] Soldano L B and Pennings E C M 1995 Optical multi-mode interference devices based on self-imaging: principles and applications *J. Lightwave Technol.* **13** 615–27